Continental Shelf Research 141 (2017) 38–50

Contents lists available at ScienceDirect

Continental Shelf Research

journal homepage: www.elsevier.com/locate/csr

Research papers

A source of CO_2 to the atmosphere throughout the year in the Maranhense continental shelf (2°30'S, Brazil)

Nathalie Lefèvre[a,*], Francisco Jose da Silva Dias[b], Audálio Rebelo de Torres Jr[b], Carlos Noriega[c], Moacyr Araujo[c], Antonio Carlos Leal de Castro[b], Carlos Rocha[d], Shan Jiang[d], J. Severino P. Ibánhez[c]

[a] IRD-LOCEAN, Sorbonne Universités (Université Pierre et Marie Curie-CNRS-MNHN), 4 place Jussieu, 75252 Paris Cedex 05, France
[b] Federal University of Maranhão - UFMA, São Luis, Brazil
[c] Departamento de Oceanografia – DOCEAN, Universidade Federal de Pernambuco – UFPE, Av. Arquitetura, s/n, Cidade Universitária, 50740-550 Recife, PE, Brazil
[d] Biogeochemistry Research Group, Geography Department, School of Natural Sciences, Trinity College, Dublin, Ireland

ARTICLE INFO

Keywords:
Carbon dioxide (CO_2)
Air-sea CO_2 flux
Organic matter
Continental shelf of Maranhão
Coastal Atlantic
Western tropical Atlantic

ABSTRACT

To reduce uncertainty regarding the contribution of continental shelf areas in low latitude regions to the air-sea CO_2 exchange, more data are required to understand the carbon turnover in these regions and cover gaps in coverage. For the first time, inorganic carbon and alkalinity were measured along a cross-shelf transect off the coast of Maranhão (North Brazil) in 9 cruises spawning from April 2013 to September 2014. On the last 4 transects, dissolved organic matter and nutrients were also measured. The highest inorganic and organic carbon concentrations are observed close to land. As a result of low productivity and significant remineralization, heterotrophy dominates along the transect throughout the year. Although the temporal variability is significantly reduced at the offshore station with carbon concentrations decreasing seaward, the fugacity of CO_2 (fCO_2) at this station remains significantly higher, especially during the wet season, than the open ocean values measured routinely by a merchant ship further west. Overall, the continental shelf is a weak source of CO_2 to the atmosphere throughout the year with an annual mean flux of 1.81 ± 0.84 mmol m^{-2} d^{-1}. The highest magnitudes of fCO_2 are observed during the wet season when the winds are the weakest. As a result, the CO_2 flux does not show a clear seasonal pattern. Further offshore, fCO_2 is significantly lower than on the continental shelf. However, the oceanic CO_2 flux, with an annual mean of 2.32 ± 1.09 mmol m^{-2} d^{-1}, is not statistically different from the CO_2 flux at the continental shelf because the wind is stronger in the open ocean.

1. Introduction

The continental shelf is an environment of strong biogeochemical activity due to the input of terrestrial material, enhanced sediment-water interactions, biological uptake and respiration and remineralization processes. Coastal waters receive terrestrial material from sediments, rivers, and groundwater discharge and as such are more affected by human activities than the open ocean. Nutrient loading and the decrease of turbidity when continental freshwater inputs mix with oceanic waters favors primary production, often leading to autotrophy. As an example, the freshwater discharge of the Amazon River causes large diatoms blooms (1996) and significantly decreases the seawater fugacity of CO_2 (fCO_2) (e.g. Cooley et al., 2007; Ibánhez et al., 2015; Körtzinger, 2003; Lefèvre et al., 2010). This mechanism is also observed with the discharge of other large rivers into the ocean (Cai et al., 2013). However, the rates of respiration and organic matter degradation can also be very high and, in some cases, they counteract the autotrophic process rates so that heterotrophy becomes the net result (Bauer and Bianchi, 2011). This is the case for many estuaries (e.g. Borges et al., 2006; Noriega and Araujo, 2014). Direct inorganic carbon input from river waters play an important role in enhancing fCO_2 of shelf waters (Jiang et al., 2008). Tidal exchange with mangroves may also raise fCO_2 in continental shelf waters (Borges et al., 2003) and is a source of dissolved inorganic carbon (Bouillon et al., 2008).

The complexity of the carbon dynamics in coastal areas has led to uncertainty regarding the role of the coastal ocean as a sink or source of CO_2 to the atmosphere and only recently it has been established that, overall, continental shelves absorb CO_2 (Chen and Borges, 2009). However, continental shelves are spatially and functionally heteroge-

* Corresponding author.
E-mail address: Nathalie.lefevre@locean-ipsl.upmc.fr (N. Lefèvre).

http://dx.doi.org/10.1016/j.csr.2017.05.004
Received 23 September 2016; Received in revised form 4 May 2017; Accepted 9 May 2017
Available online 12 May 2017

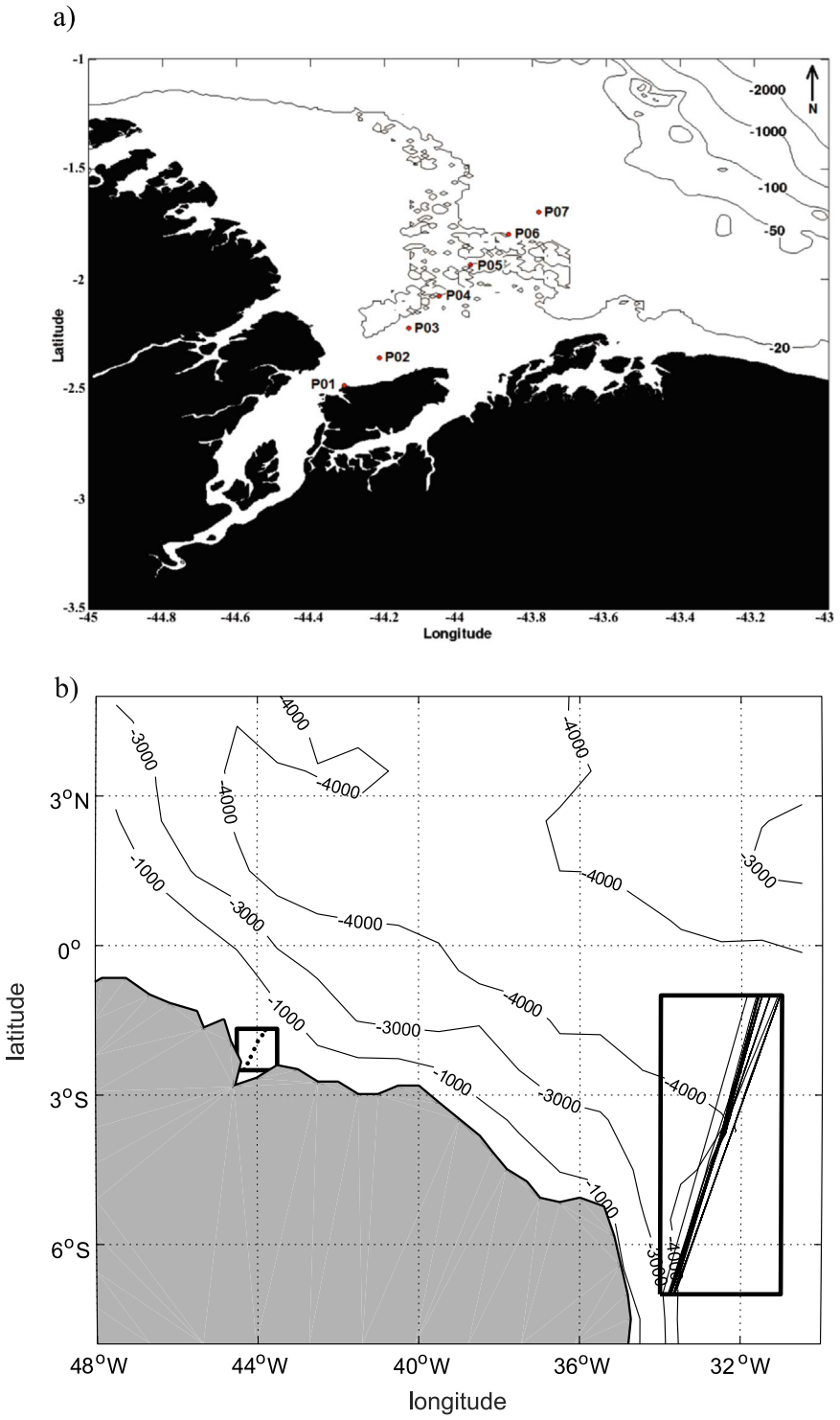

Fig. 1. a) Positions of the 7 stations sampled along the transect of the continental shelf of Maranhão ("coastal box") and voyages of the VOS line (rectangle corresponding to the oceanic box). b) Zoom on the continental shelf of Maranhão.

neous, leading Cai et al. (2006) to classify them into seven provinces. They show that while most shelves absorb atmospheric CO_2, continental shelves at low latitudes are a source of CO_2 to the atmosphere. For the western boundary current shelves, located between 30°S and 30°N, the net export of CO_2 to the atmosphere is caused by the large continental inputs of organic and inorganic carbon and the high sea surface temperature. In the tropics, mangroves are the major ecosystem at the continental margin and they are responsible for large material exchange at the land-sea interface. As highly productive systems, they export organic matter and nutrients to adjacent coastal waters and therefore exert significant control over the biogeochemical carbon cycle in the coastal region (Dittmar et al., 2006; Tait et al., 2016).

Using data from 165 estuaries and 87 continental shelf areas, Chen et al. (2013) determined the source or sink nature of CO_2 turnover and classified the resultant data according to salinity and latitudinal ranges. Although low latitude regions are less studied in comparison to coastal areas in temperate regions, some estimates were still available. For the continental shelf 0°–23.5°S, they estimate an annual CO_2 flux of 0.22 ± 0.42 mmol C m^{-2} d^{-1} (n=5). The large uncertainty of the CO_2 flux at

low latitudes is due to the very sparse data coverage (Bauer et al., 2013). In order to reduce the uncertainty regarding the contribution of continental shelf areas in low latitude regions to the air-sea CO_2 exchange flux on a global scale, a more complete understanding of carbon turnover in these shelf regions has to be developed, and this requires more data to cover gaps in coverage.

Here we present carbon data for the Maranhense continental shelf (Gulf of Maranhão), located at about 2°30'S, south of the Amazon delta (equator), in a region affected by large mangroves and continental freshwater discharge. For the first time, the alkalinity (TA) and inorganic carbon (TCO_2) concentrations were measured along a transect perpendicular to the coast between 2013 and 2014. The 9 months of sampling allow a seasonal description of this continental shelf from the point of view of carbon turnover. This dataset is completed by dissolved organic carbon (DOC), Fluorescent Dissolved Organic Matter (FDOM) and nutrient concentrations measured on the last four transects of 2014, which provide a deeper insight on the processes at play on the continental shelf. The spatial variability of the carbon parameters is assessed by comparing the coastal carbon data to measurements made in the open ocean by a merchant ship equipped with an underway fCO_2 system and during a cruise in 2014. Our work therefore contributes to improve our knowledge of the continental shelf carbon cycle at low latitudes and provides carbon data in a region of the coast of Brazil never sampled before.

2. Material and methods

2.1. Study site

The Amazonian coast, comprised by the Brazilian states of Maranhão, Pará and Amapá, contains the largest continuous mangrove system in the world, covering an area of 8900 km^2 (Kjerfve et al., 2002). The state of Maranhão is located in the north coast of Brazil and it contains about 750,000 ha of mangroves (Kjerfve and Lacerda, 1993). The macrotidal coast of Maranhão contains 500,000 ha of these mangroves, more than 30% of the total for all Brazil (Mochel and Ponzoni, 2007). Biomass may reach 280 t/ha. According to Dittmar et al. (2001), carbon export from mangroves may play a more important role than that supplied by rivers for the marine carbon system along the Brazilian coast south of the Amazon estuary.

According to the Köppen climate classification, the westernmost part of the northeastern Brazilian coast is an Am (tropical wet climate) region. The São Marcos Bay and the São José Bay form the Maranhense Gulf which includes estuaries, straits, many islands and a large mangrove forest that covers about 5414 km^2 (Souza-Filho, 2005).

The two main rivers draining the catchment area (0.09×10^6 km^2) into the system are the Pindaré and Mearim. They flow into the Bay of São Marcos with a discharge rate of 10 km^3 yr^{-1} (Jennerjahn et al., 2010). The maximum discharge occurs in March-April at the peak of the wet season that takes place from January to July. The tidal range can reach 8 m. During the period of sampling, the tidal height varied between 3.6 m in November 2013 and 6 m in March 2014.

A transect from the Bay of São Marcos comprising 7 stations (Fig. 1a) was sampled in April, August, October, November 2013, and January, March, May, July and September 2014. The westernmost longitude corresponds to station 1 in the bay of São Marcos, close to the city of São Luis, while the last station (Station 7, 97 km from station 1) is located on the continental shelf before the isobath of 50 m.

During 2013, two oceanographic cruises (April and November) were conducted in the Bay of São Marcos during the rainy and dry seasons, respectively. Each cruise lasted an average of 2 days and consisted of a total of 20 hydrographic stations distributed in four transects. CTD data (pressure, temperature and conductivity) were collected along each transect. Based on calibration data, the final precisions of the CTD data were $\pm$ 0.05 in salinity and $\pm$ 0.02 °C in temperature. The sampling rate of the CTD was 15 Hz. The data for the fluvial contribution were obtained according to Dias et al., (2011, 2013).

In order to compare the carbon system of the Gulf of Maranhão to the one operating in the open ocean, underway data on fCO_2 measured with an automated infrared system on board the Volunteer Observing Ship (VOS) line France-Brazil are used. The CO_2 system is similar to the one described by Pierrot et al. (2009) and some of the voyages of the VOS line have been described by Lefèvre et al. (2013). A total of 27 cruises were carried out between 2008 and 2014 (Fig. 1b).

The coastal region off Maranhão and the oceanic region covered by the VOS cruises are delimited by rectangles in Fig. 1b and hence represent two regions where the seasonal cycle of fCO_2 may be determined and compared. The selected oceanic region is 1241 km from the coastal region.

The ocean circulation pattern in the tropical Atlantic is mainly zonal with the South Equatorial Current (SEC) flowing westward from the coast of Africa to the coast of Brazil. Close to 14°S, the southern branch of the SEC (sSEC) splits into northern and southern components when reaching the coast of Brazil. The northern flow forms the North Brazil Undercurrent - North Brazil Current (NBUC-NBC) system, which is also fed by the central SEC (cSEC) whereas the southern flow forms the Brazil Current (Silva et al., 2009; Stramma and Schott, 1999). Studies conducted over the northern and northeastern Brazilian continental shelf have shown the existence of space-time variability in the North Brazil Current (NBC) caused by trade winds variability and the anticyclonic vortex that meanders along the adjacent ocean towards the continental shelf (Dias et al., 2013).

The Maranhense Gulf is bordered seaward by the western boundary current NBC. The NBC is a strong alongshore current that intensifies from July to August when the south-eastern trade winds blowing towards the Intertropical Convergence Zone (ITCZ), located north of the equator, become stronger. As a consequence the NBC reaches its weakest intensity during April-May (Johns et al., 1998). From November to April, the southeastern winds are weaker and the ITCZ migrates south of the equator. Within the area defined by the oceanic box in Fig. 1b, the SEC and, as the ship gets closer to the coast, the NBC are present.

2.2. Carbonate chemistry

Surface seawater samples, taken at a depth of 0.5 m, were analyzed for TCO_2 and TA. Unfortunately, several flasks were broken during transport and data are missing at some stations (Table 1). Upon collection, samples were poisoned with a saturated $HgCl_2$ solution and

Table 1
List of cruises with parameters sampled in the Gulf of Maranhão.

Transects	Dates	Sampled parameters	Sampled stations
Ma01	28–29 January 2014	TCO_2, TA	1,2,3,6,7
Ma03	27–28 March 2014	TCO_2, TA	1,4,5,6,7
		DOC, FDOM, nutrients	1,2,3,4,5,6
Ma04	11–12 April 2013	TCO_2, TA	1,2,3,4,5,6,7
Ma05	27 May 2014	TCO_2, TA	2,3,6,7
		DOC, FDOM, nutrients	1,2,3,4,5,6,7
Ma07	22–23 July 2014	TCO_2, TA	1,2,3,4,5,6,7
		DOC, FDOM, nutrients	2,3,4,6
Ma08	6–7 August 2013	TCO_2, TA	1,2,3,4,5,6,7
Ma09	23–24 September 2014	TCO_2, TA	1,2,3,4,5,6
		DOC, FDOM, nutrients	1,2,3,4,5,6,7
Ma10	1–2 October 2013	TCO_2, TA	1,2,3,4,5,6,7
Ma11	26–27 November 2013	TCO_2, TA	1,2,3,4,5,6,7

measured using an open-cell potentiometric titration following the method of Edmond (1970). Equivalent points were determined using a non-linear regression method (DOE, 1994). Certified Reference Materials (CRMs) provided by Prof. A. Dickson (Scripps Institution of Oceanography, San Diego, USA) were used for calibration. The accuracy of TCO_2 and TA is estimated at ± 3 μmol kg^{-1}. Using the CO2SYS program (Pierrot et al., 2006) and the dissociation constants of Mehrbach et al. (1973) refit by Dickson and Millero (1987), pH on the total scale and fCO_2 were calculated from TA, TCO_2, in situ temperature and salinity data.

Sea-air fluxes of CO_2 were calculated using the gas exchange coefficient (k) of Sweeney et al. (2007) and the solubility (K_W) of Weiss (1974):

$$F = k\ K_w (fCO_{2\,sw} - fCO_{2\,atm}) \quad (1)$$

Seawater fCO_2 (fCO_{2sw}) was calculated from TA and TCO_2 for the analysis of the carbon system on the continental shelf of Maranhão. To determine atmospheric fCO_2 ($fCO_{2\,atm}$), we use the monthly molar fraction of CO_2 ($xCO_{2\,atm}$) recorded at the atmospheric station of the NOAA/ESRL Global Monitoring Division (http://www.esrl.noaa.gov/gmd/ccgg/iadv/) located at Maxaranguape, Brazil (5.515°S, 35.260°W). The xCO_2 record was available until December 2013 and exhibited an increase of 2.3 ppm yr^{-1} over the period Sep 2010-Dec 2013. In order to obtain xCO_2 for 2014, the value of 2.3 ppm was added to the 2013 xCO_2 values. The $fCO_{2\,atm}$ from 2013 to 2014 was then calculated from xCO_2 with the atmospheric pressure and sea surface temperature (SST) available at the NCEP/NCAR (National Centers for Environmental Prediction/ National Center for Atmospheric Research) reanalysis project (Kalnay et al., 1996). The monthly wind speed available from the NCEP/NCAR database was converted to an altitude of 10 m to calculate the CO_2 flux. An outgassing of CO_2 is observed when the difference $\Delta fCO_2 = fCO_{2\,sw} - fCO_{2\,atm}$ is positive.

For the calculation of oceanic fluxes, oceanic and atmospheric fCO_2 measured on the VOS line were used for the region defined in Fig. 1b (oceanic box). The wind speed corresponding to this oceanic region was taken from the NCEP/NCAR database.

2.3. Dissolved nutrients, DOC, FDOM

During the sampling campaigns performed between March and September 2014 additional surface water samples were collected for nutrient and Dissolved Organic Matter (DOM) determination. These were filtered on-site with GF/F filters (Whatman, 0.7 μm average pore size) and placed on acid-washed, amber glass containers. Samples were protected from light inside a cooler box until arrival at the laboratory. There, samples were kept frozen (−20 °C) until analysis. Phosphate (PO_4^{3-}) and ammonium (NH_4^+) concentrations were determined by standard colorimetric methods (Grasshoff, 1983). Determination of nitrate (NO_3^-) plus nitrite (NO_2^-) followed the method described by Garcia-Robledo et al. (2014). Dissolved organic carbon (DOC) was determined with a Vario TOC Cube elemental analyzer after acidification of the aliquots (2 M HCl) to remove dissolved inorganic carbon.

Three-dimensional emission-excitation matrix (EEM) fluorescence of the FDOM (i.e. the DOM fraction with fluorescent properties) was measured on a Cary Varian Eclipse fluorescence spectrophotometer. Samples were first conditioned in a temperature-controlled bath at 20 °C to avoid changes to spectral intensities caused by temperature differences. Absorbance scans of the samples were used to correct the EEM spectra and thus avoid inner filter effects (Kothawala et al., 2013). The fluorescence intensity was normalized to the integrated area of Milli-Q water Raman peak and reported in Raman units (r.u.). Parallel factor (PARAFAC) analysis of the dataset obtained from different water samples obtained from the vicinity (65 samples) and including the results presented here (24 samples) was performed with the DOMFluor Toolbox for MATLAB (Stedmon and Bro, 2008). The adequacy of the selected number of components and the uniqueness of the solution was tested by Split Half Analysis and Tucker's congruence coefficients (Stedmon and Bro, 2008).

2.4. Remote sensing data

Data from the Global Precipitation Climatology Project (GPCP) (Adler et al., 2003; Xie et al., 2003) is used to characterize the regional precipitation regime. INMET (Brazilian Meteorological Institute) data are used for the precipitation close to the coast of Maranhão. The station for the INMET precipitation is located in São Luis. Climatologies employed were calculated over the period 1984–2014. Anomalies were calculated as the difference between observed values and the climatology.

Chlorophyll *a* concentrations obtained from MODIS Aqua at 4×4 km resolution are used to determine the primary production in the region. The relevant climatology is calculated from 2003 to 2014.

The SST data from MODIS Terra at 4×4 km resolution are used for calculating ocean and coastal temperature climatologies over the period 2003–2014.

2.5. Statistics

The Jarque-Bera test is used to check the normality of the data sets. When the data sets follow a normal distribution, the *t*-test is performed to determine whether the data sets come from distributions with equal means. When the normality is not verified, the Wilcoxon rank sum test (equivalent to the Mann-Whitney *U* test) is used instead. All tests are made at the 5% level.

A principal component analysis (PCA) was performed using seawater fCO_2, TCO_2, TA, pH, in situ SST, salinity and MODIS chlorophyll *a* data at each station of the nine transects to identify the main modes of variability. Data gaps were filled by linear interpolation with longitude. When station 1 or station 7 is missing, the difference between stations 1–2, or stations 6–7 calculated along the other transects is used to extrapolate the values. A matrix of 63 observations of the 7 variables is used for the analysis.

3. Results

3.1. Hydrological and biological conditions

Fig. 2 shows the seasonal climatology of precipitation (1984–2014), SST (2003–2014) and chlorophyll *a* (2003–2014) for the coastal and oceanic boxes defined in Fig. 1 as well as the mean values for each transect realized in 2013–2014. In the oceanic region, the precipitation follows the same seasonal cycle compared to the coastal region, with usually slightly lower accumulated rainfall values (Fig. 2a). The INMET data give higher rainfall during the wet season compared to the GPCP coastal data. The distributions are statistically different (paired *t*-test, p=0.004). The wet season is associated with the presence of the ITCZ located at its southernmost position in March-April (Fonseca et al., 2004). This region forms a band of high precipitation and high SST from the coast of Africa to the coast of Brazil. However, there is significantly higher precipitation at the coast of Maranhão than further east in the open ocean. The GPCP data at the coast and in the oceanic box are significantly different (paired *t*-test, p=0.03). During the sampling period, the precipitation is much lower than the climatology in the wet season except for the transect realized in May 2014.

The seasonal cycle of SST follows the seasonal cycle of precipitation with maximum temperatures (> 29 °C) observed at the peak of the wet season (Fig. 2b). The SST in the coastal region is significantly higher than further east in the open ocean (paired *t*-test, $p < 0.001$). The difference is close to 1 °C except from January to June. The SST measured during the cruises is close to the climatology except in April 2013 when the temperature is about 1 °C higher that the climatology. April 2013 is also characterized by the most reduced precipitation

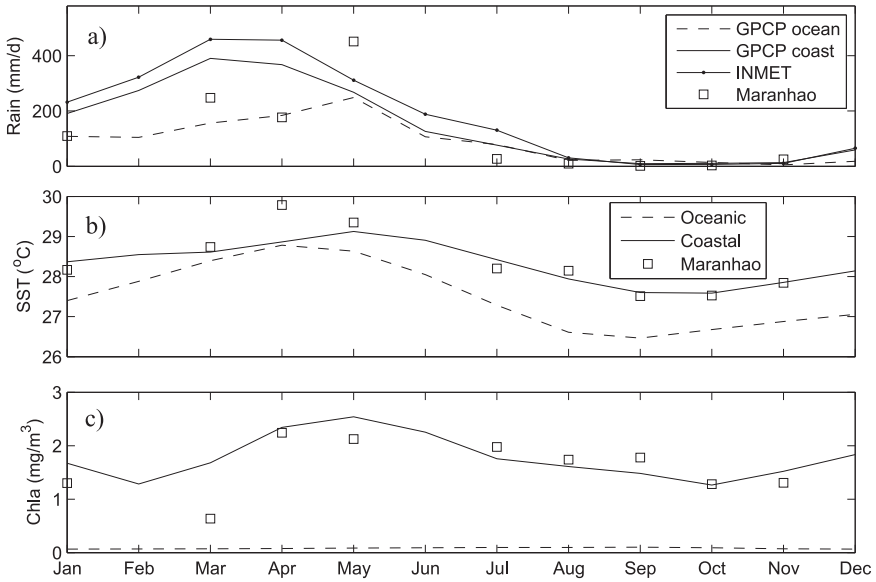

Fig. 2. Seasonal climatology of a) precipitation, b) SST and c) chlorophyll *a* for the coastal and oceanic regions. The squares correspond to the data for each transect realized in the Gulf of Maranhão in 2013–2014 (precipitation from GPCP, in situ SST, chlorophyll from MODIS Aqua).

compared to the climatology. The biological activity is stronger in the coastal region than in the open region (paired *t*-test, $p < 0.001$) but remain quite low with concentrations of chlorophyll *a* ranging from 1 to 2 mg m^{-3} (Fig. 2c).

3.2. Sea surface temperature, salinity and water masses

Temperature and salinity data measured inside the Bay of São Marcos in 2014 during the dry and wet seasons explain the main characteristics of the water masses in this region. More saline and colder waters are present during the dry season whereas, during the wet season, the water is fresher and warmer (Fig. 3). The freshwater endmember (S=0) is not encountered during the sampling in the Bay. The isohaline 30, corresponding to the transition between the estuary and the continental shelf, is observed 12 km further north during the wet season, close to station 1.

Sea surface salinity (SSS) and SST measured along the 9 transects are plotted as a function of longitude between April 2013 and September 2014, along with TA, TCO_2, chlorophyll and fCO_2 (Fig. 4).

The salinity is highly variable close to the bay of São Marcos (station 1) ranging from 25.95 to 35.95 (Fig. 4a). Over the sampling period (April 2013 to September 2014), the lowest salinities were observed in May 2014 associated with precipitation higher than climatological values. In May and July 2014 the low salinity water ($S < 29$) associated with high SST (> 28.7 °C) characterizes the mixing between estuarine water and continental shelf water. For stations 5, 6, 7 and transects realized when precipitation was low, salinity is higher (> 36.2) with lower SST (< 28 °C), which corresponds to the tropical water mass. During the wet season, in the middle of the transect (stations 2–4), salinity varies between 30–35.5 and SST between 28–29.5 °C. No correlation is observed between salinity and tidal height. The salinity data do not follow a dilution curve between freshwater and seawater along the transect, where the lowest salinity would be at station 1 and the highest salinity at station 7. Instead, the highest salinities can occur in the middle of the transect. For example, in November 2013, the highest salinity is observed at station 3 (37.35) and then it decreases slightly offshore to reach 36.59 at station 7.

The SST decreases seaward with a stronger temperature gradient from September to November. At the peak of the wet season (Mar-May), the SST difference between the first station and the last one is smaller (< 0.5 °C). As shown by the SST climatology, the seasonal SST variations are slightly lower in the coastal area. At station 1, the SST ranges from 28.49 °C to 29.41 °C while SST varies from 27.66 °C to 29.17 °C at station 7. Taking into account all the transects, the mean SST is 28.52 ± 0.54 °C.

3.3. Alkalinity and inorganic carbon

The alkalinity distribution follows the salinity variations with a general increase from the bay of São Marcos towards the ocean and large alkalinity variations (> 330 µmol kg^{-1}) at station 1 (Fig. 4c). Alkalinity concentrations range from 2082 to 2444 µmol kg^{-1} with the lowest alkalinities associated with the lowest salinities. Nearshore values are usually smaller than at the open ocean station 7 except in November 2013 when nearshore alkalinity is higher (Table 2). A strong alkalinity-salinity correlation is observed at the first 3 stations ($r^2 > 0.92$). Over the whole transect, the correlation is slightly lower ($r^2=0.85$).

The TCO_2 variability exhibits similar patterns to alkalinity with higher variability closer to the coast and variations lower than 50 µmol kg^{-1} at station 7 (Fig. 4d, Table 2). The values range from 1875 to 2132 µmol kg^{-1}. The lowest TCO_2 concentrations are observed from May to August at stations 1 and 2 and are associated with the lowest salinities and TA. At the first three stations, TCO_2 is strongly correlated with TA (r^2 ranging from 0.94 to 0.97) and less with salinity (r^2 ranging from 0.86 to 0.90).

3.4. Chlorophyll a, dissolved nutrients and seawater fugacity of CO_2

Following the sampling transect, chlorophyll *a* concentrations are higher nearshore and decrease offshore (Fig. 4e). The highest value was observed in July 2014 at station 1 and is associated with the lowest salinity measured. Nearshore concentrations range from 3.25 to 4.71 mg m^{-3} whereas, at station 7, the chlorophyll *a* exhibits much lower concentrations and smaller variability with values between 0.22 and 0.51 mg m^{-3}. The highest concentrations of DIN and PO_4^{3-} are measured nearshore and decrease seaward, following the same pattern as the chlorophyll. NH_4^+ concentrations are zero except in September 2014 at station 1 (0.14 µM) and in May 2014 at station 2 (1.5 µM).

The fugacity of CO_2 in seawater decreases from the coast to the open ocean and exhibits a larger variability nearshore (Fig. 4f). The highest fCO_2 value (686 µatm) is observed in March 2014 close to the

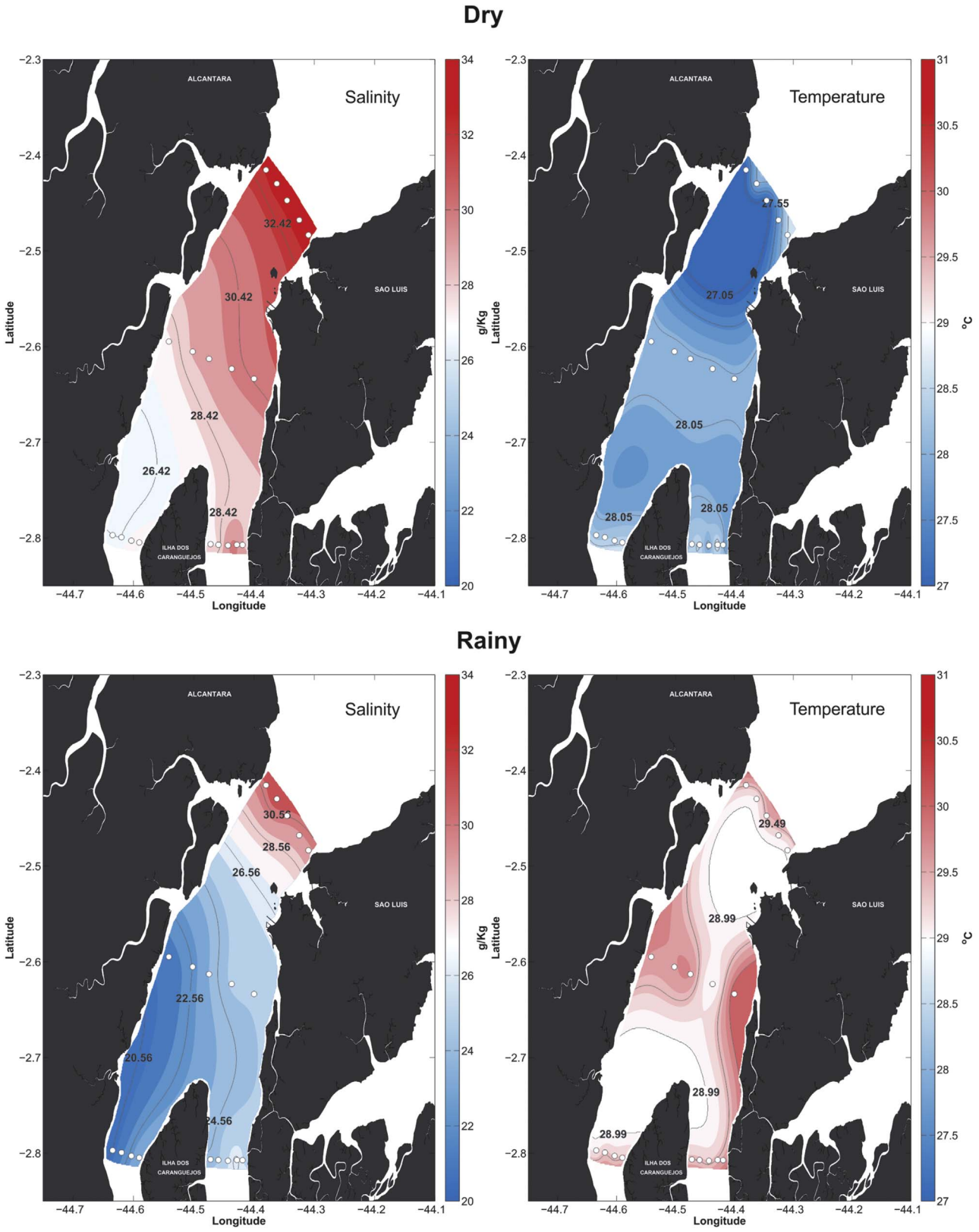

Fig. 3. Distribution of temperature and salinity of the São Marcos Bay for the wet and dry seasons in 2014.

city of São Luis (station 1). The range of fCO_2 is over 200 µatm at this location. Further offshore, the variability is much lower but still quite large with a range of about 80 µatm at station 7. Higher fCO_2 tend to occur during the wettest months (Mar-Apr) whereas the dry season is usually characterized by lower fCO_2 values.

3.5. FDOM and DOC

FDOM and DOC were measured during the last 4 transects of March, May, July and September 2014. Four FDOM components were identified: Components 1 and 2 (C1, C2) have characteristic emission

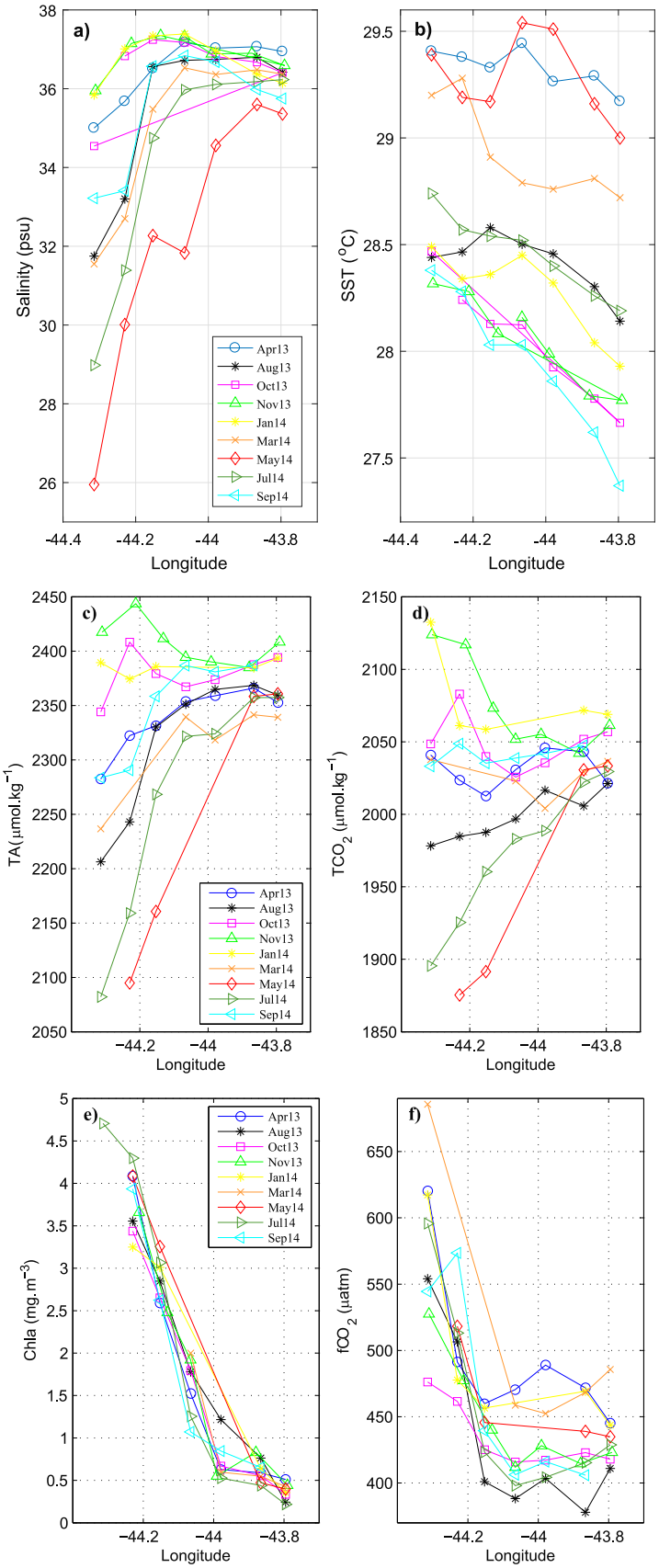

Fig. 4. Distribution of a) SSS, b) SST, c) TA, d) TCO_2, e) chlorophyll *a* and f) seawater fCO_2 as a function of longitude for each cruise off the coast of Maranhão, Brazil.

Table 2
Nearshore (station 1) and open ocean (station 7) end-members of salinity (S), alkalinity (TA in µmol kg^{-1}) and inorganic carbon (TCO_2 in µmol kg^{-1}).

Month	Nearshore end-members				Open ocean end-members			
	S	TA	TCO_2	fCO_2	S	TA	TCO_2	fCO_2
Jan 2014	35.84	2389	2132	617	36.14	2394	2069	444
Mar 2014	31.55	2237	2038	686	36.37	2339	2036	486
Apr 2013	35.00	2282	2041	620	36.94	2353	2021	445
May 2014					35.36	2361	2033	435
Jul 2014	28.98	2082	1895	596	36.23	2357	2029	429
Aug 2013	31.75	2206	1978	554	36.42	2360	2021	411
Sep 2014	33.22	2284	2033	544				
Oct 2013	34.54	2344	2048	476	36.41	2394	2057	418
Nov 2013	35.95	2417	2124	528	36.59	2394	2052	412

(excitation) wavelengths (i.e. the wavelength where the maximum fluorescence intensity occurs) of 474 (< 250/360) nm and 410 (< 250/325) nm respectively, typical of humic-like FDOM components (Coble, 1996). Components 3 and 4 (C3, C4) have emission (excitation) wavelengths of 342 (< 250/300) and 302 (< 275) nm respectively, similar to pure Tryptophan (340 nm emission, 278 nm excitation; Kowalczuk et al., 2003) and Tyrosine (310 nm emission, 275 nm excitation; Kowalczuk et al., 2003) amino acids (Fig. S1).

The sum of the fluorescence intensity of the four FDOM components is correlated with DOC (r^2=0.56) and shows a decrease seaward.

The FDOM and DOC distributions show higher values nearshore and are associated with lower salinity (Fig. 5). DOC concentrations range from 113 to 210 µM. Along the transect, the highest DOC concentrations are systematically observed in May 2014 concurrently with the strong positive anomaly of rainfall registered in the area (Fig. 3a). DOC and the humic-like components of the FDOM pool appeared significantly correlated to SSS and NO_3^- during the four sampling campaigns ($r^2 > 0.57$; $p < 0.005$; n=24). The two humic-like FDOM components were also significantly correlated with fCO_2 (C1: r^2=0.83, $p < 0.001$; C2: r^2=0.81, $p < 0.001$). The protein-like FDOM components also showed correlation with NO_3^- ($r^2 > 0.19$; $p < 0.05$; n=24) but not with salinity ($p > 0.05$).

3.6. Sea-air CO_2 flux

Using monthly atmospheric fCO_2 and wind data, the monthly flux of CO_2 is calculated for each of the 9 transects and compared to the open ocean CO_2 flux (Fig. 6). Seawater fCO_2 tends to be higher during the wet season and this pattern is also observed on ΔfCO_2 as atmospheric fCO_2 has a much smaller variability (~4 µatm) than oceanic fCO_2 (Fig. 6a). It results in a large variability of ΔfCO_2 ranging from 50 µatm (October) to 130 µatm (March). Further offshore, ΔfCO_2 exhibits significantly smaller values than those on the continental shelf on a monthly basis (unpaired *t*-test, $p < 0.001$). Averaging all the values leads to a ΔfCO_2 of 33 ± 9 µatm whereas a mean of 85 ± 27 µatm is observed on the continental shelf.

The wind speed in the open ocean is stronger than on the continental

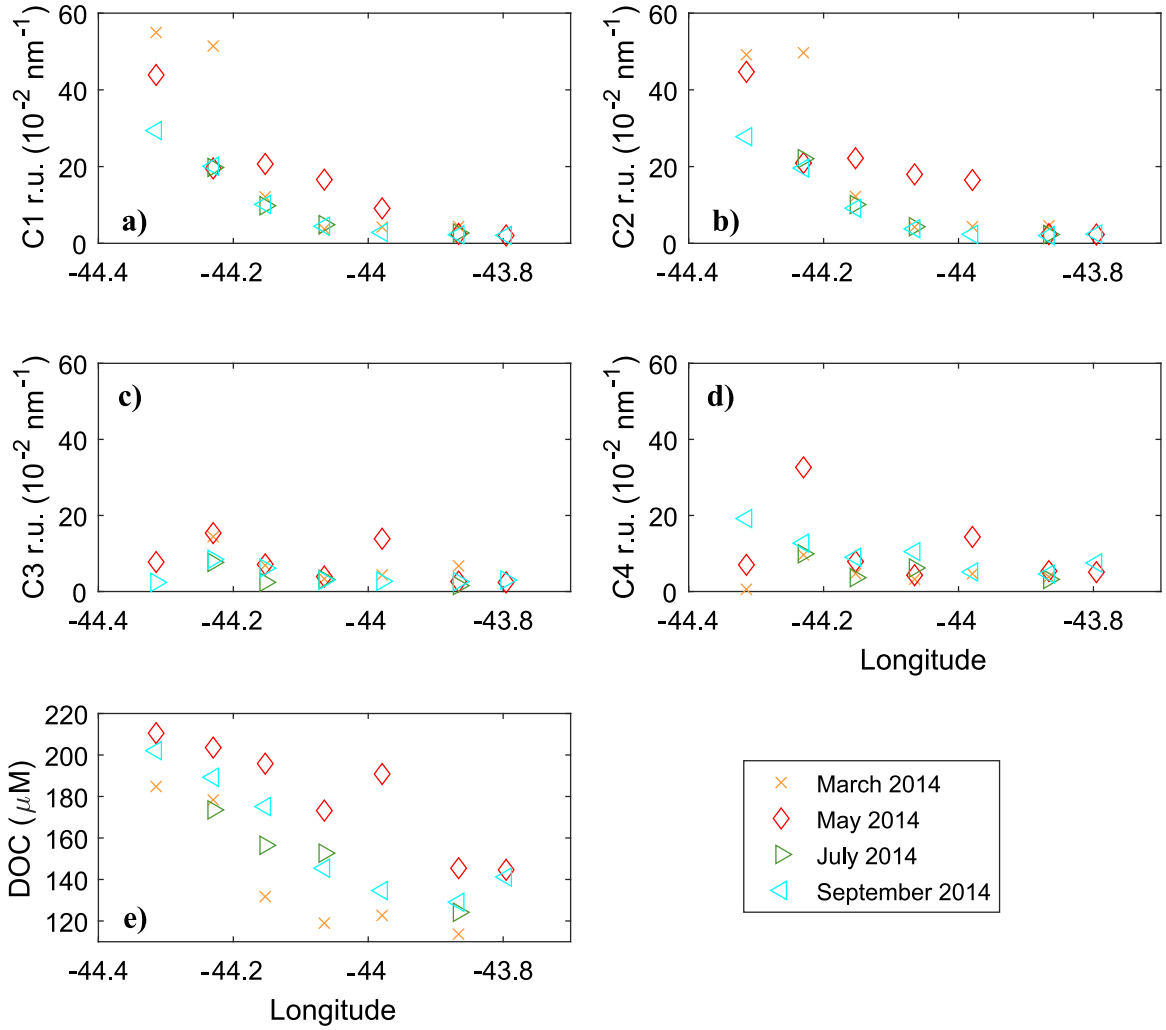

Fig. 5. Components a) C1, b) C2, c) C3 and d) C4 of FDOM, and e) DOC as a function of longitude.

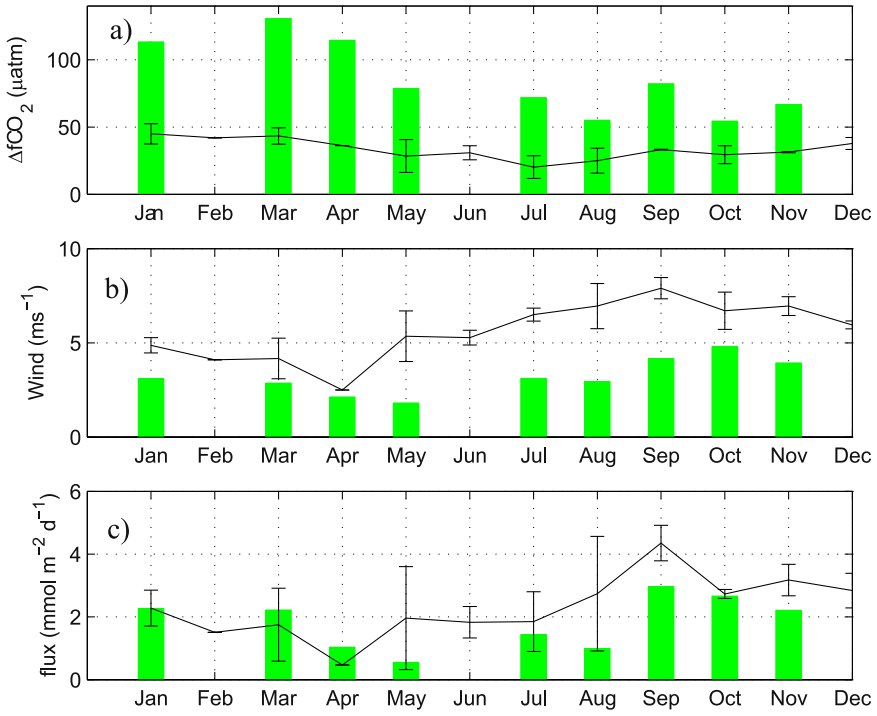

Fig. 6. a) Monthly distributions of ΔfCO_2, b) wind speed and c) CO_2 flux. The vertical bars represent the data on the continental shelf of Maranhão and the line with the standard deviation corresponds to the mean of the VOS data for each voyage.

shelf (unpaired *t*-test, $p < 0.001$) with values over 6 m s^{-1} (Fig. 6b) and an annual mean of 5.7 ± 1.4 m s^{-1} versus 3.20 ± 0.96 m s^{-1} on the continental shelf.

The continental shelf is a source of CO_2 to the atmosphere (Fig. 6c) with outgassing occurring throughout the year as ΔfCO_2 is always positive. No relation is found between the CO_2 flux and ΔfCO_2 but the sea-air CO_2 flux is strongly correlated with the wind speed (r^2 =0.72). Offshore, the strongest outgassing is observed in September-October when the wind is stronger (Fig. 6c). The annual mean of the sea-air CO_2 flux (2.32 ± 1.09 mmol m^{-2} d^{-1}) is not statistically different from the annual mean of the CO_2 flux of the continental shelf (1.81 ± 0.84 mmol m^{-2} d^{-1}), which suggests that the stronger wind counterbalances the lower ΔfCO_2 measured offshore.

3.7. Principal components analysis

The PCA identifies 3 leading modes that account for 97% of the variability encountered. The first mode (57%) opposes fCO_2, chlorophyll and SST to pH, TCO_2, TA and salinity as shown by the bi-plot of the first two factors (Fig. 7a). The three principal components (PC) are plotted as a function of the seven stations of each transect from January to November (Figs. 7b, 7c, 7d). The factor loadings of the first three modes are given in Table S1. The first principal component (PC1) highlights the cross-shelf variability with strong differences observed at stations 1 and 2 compared to stations 3–7 (Fig. 7b). The second mode represents 29% and is dominated by the May, July and August transects (Fig. 7c) that are characterized by lower TCO_2 throughout the whole transect (Fig. 4b). PC3 (11%) is characterized by the opposition between the March-May period and the July-January period (Fig. 7d). The SST dominates this mode, with higher SST during the wet season and a stronger SST in April compared to the climatology and other months (Fig. 2b).

4. Discussion

4.1. Processes affecting the spatial variability on the continental shelf

The Maranhense Gulf receives inputs of organic and inorganic carbon from terrestrial sources (river, estuary, mangrove, pore-water and groundwater) and the relatively high salinity (> 25) throughout the year suggests a strong influence of open ocean waters in mixing, as usually observed in continental shelves (Chen et al., 2013). Each transect exhibits the highest values of fCO_2, chlorophyll *a*, DOC, FDOM, DIN, PO_4^{3-} and SST nearshore (at station 1) with a decrease seaward (station 7), pointing at the continental influence over these parameters. Overall, the PCA highlights the difference between the nearshore stations 1 and 2 and the other stations. The cross-shelf variability of the carbon parameters is therefore the dominant mode of variability along the transect.

The chlorophyll *a* decrease offshore is strongly correlated to an increase of TCO_2 from May to August (r^2 between 0.85 and 0.99). However, primary production is not strong enough to drawdown CO_2 below atmospheric levels. On the contrary, very high fCO_2 are observed with high chlorophyll concentrations. The positive correlation of fCO_2 with chlorophyll *a* clearly suggests that photosynthesis is not the dominant process underpinning the fCO_2 variations. Even in May 2014 and August 2013, when TCO_2 and chlorophyll *a* are inversely correlated, fCO_2 and chlorophyll *a* are not. In the other months, no correlation was found except in November when TCO_2 and chlorophyll *a* both decrease seaward (r^2=0.87). With the exception of the Amazon River mouth, in northern Brazil, due to low river discharge and nutrient-poor oceanic waters, the productivity is low and relies on recycling of nutrients from resuspension of sediments (Jennerjahn et al., 2010).

According to Jiang et al., (2008, 2013), on the continental shelf, the large oceanic TCO_2 pool may mask the inputs from terrestrial sources

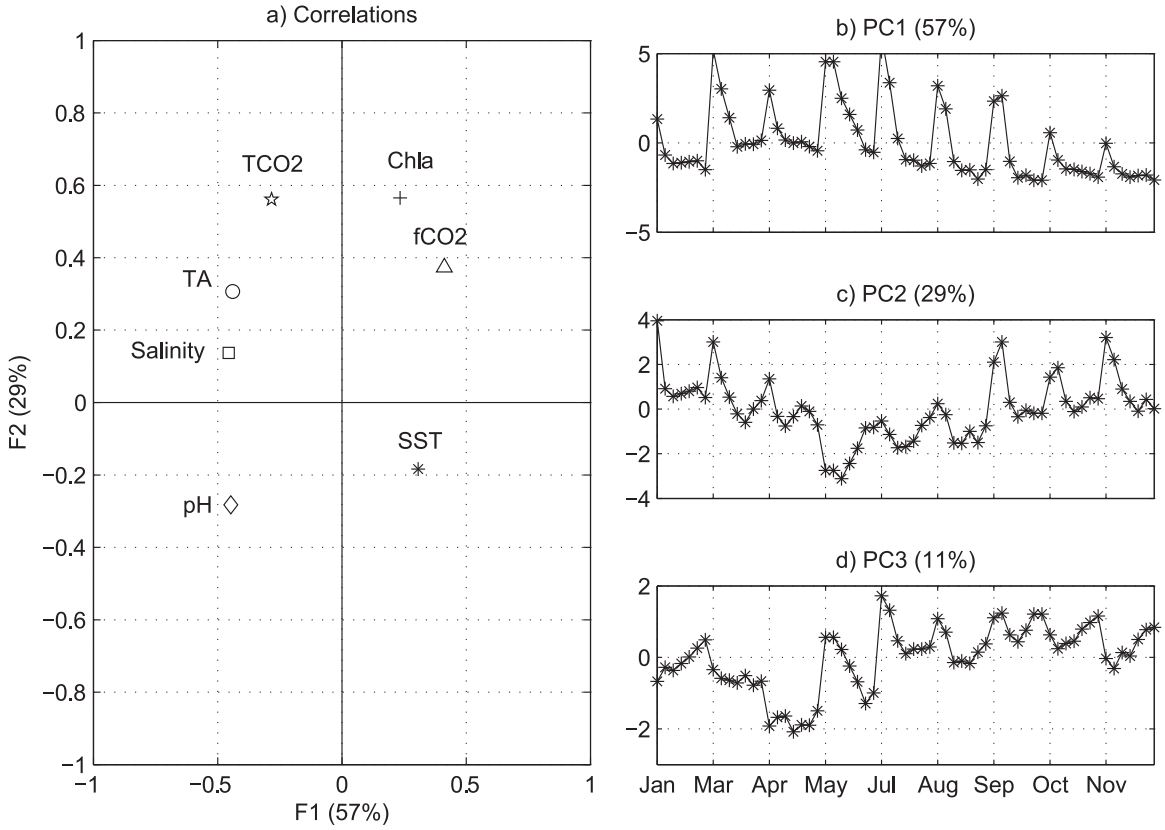

Fig. 7. Principal Component (PC) Analysis results. a) Bi-plot of the first two factors, b) PC1, c) PC2, d) PC3 as a function of the 63 observations (7 stations per transect).

whereas inputs of organic carbon from terrestrial sources can be readily detected on the seaward end.

Fluorescence spectra are used to identify the source of dissolved organic matter. Both humic-like FDOM components identified by PARAFAC modeling (C1 and C2) present characteristics similar to components commonly identified in natural waters. C2 is similar to the so-called peak M (Coble, 1996), a freshly produced humic-like FDOM compound associated with microbial metabolism in both freshwater and marine environments (Parlanti et al., 2000; Zhang et al., 2009), while C1 has a more complex structure (higher characteristic emission wavelength compared to C2, associated to higher aromaticity (Coble, 1996)) and is related to terrestrial organic matter inputs to the sea (Clark et al., 2002; Murphy et al., 2008). Although they can be produced by organic matter mineralization (e.g. Parlanti et al., 2000) or consumed by benthic metabolism under certain circumstances such as DIN pollution of pore water (Ibánhez and Rocha, 2014), both humic-like components are generally considered refractory compounds. In the Maranhão shelf waters, both FDOM components co-varied with salinity and NO_3^-, strongly suggesting its conservative distribution and terrestrial origin. In contrast to C1 and C2, the protein-like FDOM (C3 and C4) components did not show evidence of a conservative distribution as denoted by the lack of correlation with salinity. These components correspond to a low molecular weight, highly labile DOM fraction with short residence times in aquatic ecosystems (Stubbins et al., 2014), previously related to the amino acid content in marine waters (Yamashita and Tanoue, 2003). Protein-like FDOM components showed their highest concentrations nearshore but a significant enrichment is observed in the middle of the transect coincident with the measured salinity maximum. Both primary production and microbial mineralization of organic matter can produce protein-like FDOM (Wada and Hama, 2013). Although some correlation of these components is observed with chlorophyll *a* (r^2=0.52 for C3, r^2=0.31 for C4), as oligotrophic conditions are found in the outer sampling stations, mineralization of organic matter seems to be the dominant process for the production of FDOM in the middle of the transect, justifying its localized enrichment by comparison to surrounding waters. Benthic metabolism could also contribute to the high concentrations of DOC and FDOM nearshore, at shallow depths.

Following the rapid decrease of organic carbon and fCO_2 values from station 1 to station 7, about 97 km from station 1, we examine whether oceanic conditions are reached at the most offshore station of the transect.

4.2. Continental shelf – open ocean variability

As fCO_2 was measured on board a merchant ship further offshore (France-Brazil line), the fCO_2 at station 7 is compared to oceanic fCO_2 values obtained over several seasons and years. The SST in the continental shelf is slightly higher than the SST in the open ocean. In

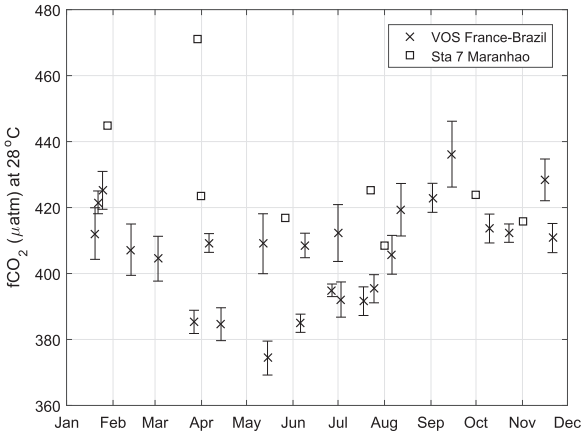

Fig. 8. Comparison of seawater fCO_2 between station 7 and the mean offshore values (VOS line France-Brazil) at a constant temperature of 28 °C.

order to remove the effect of SST on fCO_2, fCO_2 was normalized at a constant temperature of 28 °C to compare the coastal and open ocean values. Despite the significant decrease in fCO_2 observed from station 1–7, the values at the latter remain above the oceanic fCO_2 (Fig. 8, Wilcoxon rank sum test, $p < 0.01$).

Although the concentrations of DOC decrease seaward, all the 4 transects have levels of DOC higher than 120 μM (Fig. 5e). For comparison, Hanssell et al. (2009) give a typical DOC range of concentration of 60–80 μM for marine waters, which indicates enrichment of DOC occurs on the continental shelf of Maranhão. Southeast of the Amazon estuary, Dittmar et al. (2006) measured DOC concentrations decreasing from 196 μM nearshore, in the mangrove-fringed estuaries, to 64 μM offshore. The concentrations observed here are slightly higher with a maximum of 210 μM at station 1 to a minimum of 110 μM at station 7 (Fig. 5e). The mean DOC at station 7 is 131 ± 15 μM and is well above the typical open ocean values.

The production and accumulation of protein-like FDOM components in the middle of the transect, where chlorophyll *a* remained at very low levels, suggest autochthonous processing of organic matter. Mangroves are considered the main sources of terrigenous DOC to the ocean and have a known influence on the North Brazilian shelf (Dittmar et al., 2006). The complex matrix of animal burrowing together with tidal pumping, advection and convection promote extensive pore-water exchange in mangrove sediments and revealed these as a highly relevant DIC and DOC export vector to the continental shelf (Tait et al., 2016). Due to the low depth of the sampled shelf waters (< 50 m), benthic metabolism could act also as a significant source of DOC and DIC to the studied area, enhanced by the large tidal range and the strong alongshore currents (e.g. Chipman et al., 2010; Holcombe et al., 2001).

4.3. Drivers of the carbonate system on temporal scale

During the wet season, the SST is higher (unpaired *t*-test, $p < 0.001$) and the salinity is lower (Wilcoxon rank sum test, $p < 0.05$) than during the dry season. The highest fCO_2 values are observed during the wet season and even after normalizing to a constant temperature, fCO_2 is still higher than during the dry season (Wilcoxon rank sum test, $p < 0.05$). However, because the winds are weaker during this season (unpaired *t*-test, $p < 0.001$), the CO_2 flux is not significantly different between wet and dry seasons (unpaired *t*-test, p=0.24). The continental shelf is a weak source of CO_2 to the atmosphere throughout the year. Our sea-air flux estimate is higher than the 0.22 ± 0.42 mmol m^{-2} d^{-1} reported by Chen et al. (2013) for 5 continental shelves in the latitudinal band 0°–23.5°S with only one in Brazil at 25°S. Cai et al. (2006) who divided the continental shelves into provinces give an estimate of 12 g C m^{-2} a^{-1} for the western boundary currents shelves. This corresponds to a source of 2.7 mmol m^{-2} d^{-1}, which is closer to our estimate of 1.81 ± 0.84 mmol m^{-2} d^{-1}.

Both TA and TCO_2 have seasonal variations opposite to fCO_2 variations with significantly lower concentrations during the wet season (Wilcoxon rank sum test, $p < 0.05$). Alkalinity is strongly correlated with salinity (r^2=0.84). However, the biological activity as inferred from the chlorophyll *a* concentrations is not different between the two seasons (unpaired *t*-test, p=0.9) and is relatively low. The Northeast is known to be the least productive region of the Brazilian coast with primary production of the NBC beyond the shelf between < 0.1 and 0.2 g C m^{-2} d^{-1} (Jennerjahn et al., 2010). Overall fCO_2 is weakly correlated with TA (r^2=0.21) and not at all with TCO_2 while TCO_2 and TA are correlated (r^2=0.75). This suggests that low TA and high SST explain the high fCO_2 during the wet season.

The effect of precipitation on carbon parameters can be seen in May 2014 compared to April 2013 (Figs. 4 and 5). April 2013 is characterized by a strong deficit of rainfall compared to the climatology (Fig. 3a), which explains why salinity remains above 35 along the whole transect. On the contrary, higher precipitation in May 2014 explains the lowest salinities observed and the strongest enrichment in DOC found. However, no correlation is observed between salinity and tides or river discharge, which suggests that river inputs are limited and do not control this region. Moreover, as oceanic circulation is dominated by NBC, no Amazon River influence is observed on the continental shelf of Maranhão. The impact of a strong alongshore current was also observed on the export of material from mangroves along the coast of Brazil but further south (8–24°S) where the Brazil Current (BC) southward flow is dominant (Jennerjahn and Ittekkot, 2002). Like the coast of Maranhão, this region is characterized by dense mangrove vegetation and small rivers. Because of the alongshore currents, mangrove-derived organic matter is restricted to the vicinity of the source.

5. Conclusions

The continental shelf of Maranhão was sampled for the first time with analyses of TA, TCO_2, fCO_2, chlorophyll, DOC, FDOM and nutrients on a cross-shelf transect between 2013 and 2014. Terrestrial inputs are evidenced by the higher concentrations observed nearshore, close to the city of São Luis. The highest chlorophyll *a* values were observed close to the coast, but are relatively low (3–4 mg m^{-3}) and decrease rapidly seaward. The same pattern is observed with fCO_2 but the values observed at the offshore station are higher than further west in the open ocean. The freshwater supply to the continental shelf was quite limited, as revealed by the salinity data. This is explained by the reduced precipitation in 2013–2014 compared to the climatological mean and the presence of the strong alongshore North Brazil Current. However, despite the reduced freshwater supply in 2013–2014, both inorganic and organic carbon enrichment is evidenced on the continental shelf compared to the open ocean. A strong correlation is observed between fCO_2 and the two humic-like FDOM components, indicating terrestrial influence over the carbon system in these waters. The low productivity and the organic and inorganic carbon supply explain the heterotrophy observed throughout the year. The shelf is a weak source of CO_2 without clear seasonality because of high fCO_2 during the wet season when the winds are weaker. The CO_2 flux of 1.81 ± 0.84 mmol m^{-2} d^{-1} for this region is within the published range of values for low latitudes and western boundary current shelves.

Acknowledgments

We acknowledge support from AIRD-FAPEMA BIOAMAZON Project (01739/13) and the INCT AmbTropic- Brazilian National Institute of Science and Technology for Tropical Marine Environments, CNPq/FAPESB (grants 565054/2010-4 and 8936/2011). We also acknowledge the support of the Laboratório de Química Marinha (LOQUIM, UFPE) for kindly providing reagents and spectrophotometer time for nutrient analysis. The France-Brazil VOS line has been funded and maintained by the European Integrated Projects CARBOOCEAN (contract 511176-2), CARBOCHANGE (grant agreement 264879), AtlantOS (grant agreement 633211) and the Institut de Recherche pour le Développement (IRD). Sea surface salinity data derived from thermosalinograph instruments installed onboard voluntary observing ships were collected, validated, archived, and made freely available by the French Sea Surface Salinity Observation Service (http://www.legos.obs-mip.fr/observations/sss/). Seawater samples were analyzed for TCO_2 and TA by the SNAPO-CO_2 at LOCEAN in Paris. Precipitation data from the Global Precipitation Climatology Project (GPCP) and chlorophyll concentrations from MODIS Aqua 4 km were downloaded from the Giovanni online data system, developed and maintained by the NASA Goddard Earth Sciences (GES) Data and Information Services Center (DISC). We also acknowledge the TRMM mission scientists and associated NASA personnel for production of the data used in this research effort. TMI data are produced by Remote Sensing Systems and sponsored by the NASA Earth Science and REASoN

DISCOVER project. They are available at: http://www.remss.com.

Appendix A. Supplementary material

Supplementary data associated with this article can be found in the online version at doi:10.1016/j.csr.2017.05.004.

References

Adler, R.F., Huffman, G.J., Chang, A., Ferraro, R., Xie, P., Janowiak, J., Rudolf, B., Schneider, U., Curtis, S., Bolvin, D., Gruber, A., Susskind, J., Arkin, P., Nelkin, E., 2003. The version 2 Global precipitation Climatology Project (GPCP) monthly precipitation analysis (1979-present). J. Hydrometeor. 4, 1147–1167.

Bauer, J.E., Bianchi, T.S., 2011. Dissolved organic carbon cycling and transformation. In: Wolanski, E., McLusky, D.S. (Eds.), Treatrice on Estuarine and Coastal Science. Academic Press, Waltham, 4594.

Bauer, J.E., Cai, W.-J., Raymond, P.A., Bianchi, T.S., Hopkinson, C.S., Regnier, P.A.G., 2013. The changing carbon cycle of the coastal ocean. Nature 504, 61–70. http://dx.doi.org/10.1038/nature12857.

Borges, A.V., Djenidi, S., Lacroix, G., Théate, J., Delille, B., Frankignoulle, M., 2003. Atmospheric CO_2 flux from mangrove surrounding waters. Geophys. Res. Lett. 30 (11). http://dx.doi.org/10.1029/2003GL017143.

Borges, A.V., Schiettecatte, L.-S., Abril, G., Delille, B., Gazeau, F., 2006. Carbon dioxide in European coastal waters. Estuar. Coast. Shelf Sci. 70, 375–387.

Bouillon, S., Borges, A.V., Castañeda-Moya, E., Diele, K., Dittmar, T., Duke, N.C., Kristensen, E., Lee, S.Y., Marchand, C., Middelburg, J.J., Rivera-Monroy, V.H., Smith III, T.J., Twilley, R.R., 2008. Mangrove production and carbon sinks: a revision of global budget estimates. Gl. Biogeoch. Cycles, 22, doi:10.1029/2007GB003052.

Cai, W.-J., Dai, M., Wang, Y., 2006. Air-sea exchange of carbon dioxide in ocean margins: a province-based synthesis. Geophys. Res. Lett., 33. http://dx.doi.org/10.1029/2006GL026219.

Cai, W.-J., Chen, C.T.A., Borges, A.V., 2013. Carbon dioxide dynamics and fluxes in coastal waters influenced by river plumes. In: Bianchi, T.S., Allison, M.A., Cai, W.-J. (Eds.), Biogeochemistry Dynamics at Major River-Coastal Interfaces. Cambridge Press.

Chen, C.-T.A., Borges, A.V., 2009. Reconciling opposing views on carbon cycling in the coastal ocean: continental shelves as sinks ans near-shore ecosystems as sources of atmospheric CO_2. Deep-Sea Res. II 56, 578–590.

Chen, C.-T.A., Huang, T.-H., Chen, Y.-C., Bai, Y., He, X., Kang, Y., 2013. Air-sea exchanges of CO_2 in the world's coastal seas. Biogeosciences 10, 6509–6544, (doi:6510.5194/bg-6510-6509-2013).

Chipman, L., Podgorski, D., Green, S., Kostka, J., Cooper, W., Huettel, M., 2010. Decomposition of plankton-derived dissolved organic matter in permeable coastal sediments. Limnol. Oceanogr. 55, 867–871.

Clark, C.D., Jimenez-Morais, J., Jones, G., Zanardi-Lamardo, E., Moore, C.A., Zika, R.G., 2002. A time-resolved fluorescence study of dissolved organic matter in a riverine to marine transition zone. Mar. Chem. 78, 121–135.

Coble, P.G., 1996. Characterization of marine and terrestrial DOM in seawater using excitation-emission matrix spectroscopy. Mar. Chem. 51, 325–346.

Cooley, S.R., Coles, V.J., Subramaniam, A., Yager, P.L., 2007. Seasonal variations in the Amazon plume-related atmospheric carbon sink. Gl. Biogeoch. Cycles 21, doi:10.1029/2006GB002831.

Dias, F.J.S., Lacerda, L.Dd, Marins, R.V., de Paula, F.C.F., 2011. Comparative analysis of rating curve and ADP estimates of instantaneous water discharge through estuaries in two contrasting Brazilian rivers. Hydrol. Process. 25, 2188–2201.

Dias, F.J.S., Castro, B.M., Lacerda, L.Dd, 2013. Continental shelf water masses off the Jaguaribe River (4S), northeastern Brazil. Cont. Shelf Res. 66, 123–135.

Dickson, A.G., Millero, F.J., 1987. A comparison of the equilibrium constants for the dissociation of carbonic acid in seawater media. Deep Sea Res. 34, 1733–1743.

Dittmar, T., Lara, R.J., Kattner, G., 2001. River or mangrove? Tracing major organic matter sources in tropical Brazilian coastal waters. Mar. Chem. 73, 253–271.

Dittmar, T., Hertkorn, N., Kattner, G., Lara, R.J., 2006. Mangroves, a major source of dissolved organic carbon to the oceans. Gl. Biogeoch. Cycles, 20, doi:10.1029/2005GB002570.

DOE, 1994. Handbook of methods for the analysis of the various parameters of the carbon dioxide system in sea water. ORNL/CDIAC-74, Oak Ridge, USA, A.G. Dickson & C. Goyet, eds.

Edmond, J.M., 1970. High precision determination of titration alkalinity and total carbon dioxide content of seawater by potentiometric titration. Deep Sea Res. 17, 737–750.

Fonseca, C.A., Goni, G.J., Johns, W.E., Campos, 2004. Investigation of the North Brazil current retroflection and North Equatorial Countercurrent variability. Geophys. Res. Lett., 31. http://dx.doi.org/10.1029/2004GL020054.

Garcia-Robledo, E., Corzo, A., Papaspyrou, S., 2014. A fast and direct spectrophotometric method for the sequential determination of nitrate and nitrite at low concentrations in small volumes. Mar. Chem.. http://dx.doi.org/10.1016/j.marchem.2014.1003.1002.

Grasshoff, K., 1983. In: Grasshoff, K., Ehrhardt, M., Kremling, K. (Eds.), Methods of Seawater Analysis2nd edition. Verlag Chemie, Weinheim, Germany, 634.

Hanssell, D.A., Carlson, C.A., Repeta, D.J., Schlitzer, R., 2009. Dissolved organic matter in the ocean. Oceanography 22, 202–211.

Holcombe, B.L., Keil, R.G., Devol, A.H., 2001. Determination of pore-water dissolved organic carbon fluxes from Mexican margin sediments. Limnol. Oceanogr. 46, 298–308.

Ibánhez, J.S.P., Rocha, C., 2014. Effects of recirculation of seawater enriched in inorganic nitrogen on dissolved organic carbon processing in sandy seepage face sediments. Mar. Chem.. http://dx.doi.org/10.1016/j.marchem.2014.1009.1012.

Ibánhez, J.S.P., Diverrès, D., Araujo, M., Lefèvre, N., 2015. Seasonal and interannual variability of sea-air CO_2 fluxes in the tropical Atlantic affected by the Amazon River plume. Gl. Biogeoch. Cycles, 29, doi:10.1002/2015GB005110.

Jennerjahn, T.C., Ittekkot, V., 2002. Relevance of mangroves for the production and deposition of organic matter along tropical continental margins. Naturwissenschaften 89, 23–30. http://dx.doi.org/10.1007/s00114-00001-00283-x.

Jennerjahn, T.C., Knoppers, B.A., de Souza, W.F.L., Carvalho, C.E.V., Mollenhauer, G., Hübner, M., Ittekkot, V., 2010. The tropical Brazilian continental margin. In: Liu, K.-K., Atkinson, L., Quiñones, R., Talaue-McManus, L. (Eds.), Carbon and Nutrient Fluxes in Continental Margins. Springer-Verlag.

Jiang, L.-Q., Cai, W.-J., Wang, Y., 2008. A comparative study of carbon dioxide degassing in river and marine-dominated estuaries. Limnol. Oceanogr. 53, 2603–2615.

Jiang, L.-Q., Cai, W.-J., Wang, Y., Bauer, J.E., 2013. Influence of terrestrial inputs on continental shelf carbon dioxide. Biogeosciences 10, 839–849, (doi:810.5194/bg-5110-5839-2013).

Johns, W.E., Lee, T.N., Beardsley, R.C., Candela, J., Limeburner, R., Castro, B., 1998. Annual Cycle and Variability of the North Brazil Current. J. Phys. Oceano. 28, 103–128.

Kalnay, E., Kanamitsu, M., Kistler, R., Collins, W., Deaven, D., Gandin, L., Iredell, M., Saha, S., White, G., Woollen, J., Zhu, Y., Chelliah, M., Ebisuzaki, W., Higgins, W., Janowiak, J., Mo, K., Ropelewski, C., Wang, J., Leetmaa, A., Reynolds, R., Jenne, R., Joseph, D., 1996. The NCEP/NCAR 40-year reanalysis project. Bull. Am. Meteorol. Soc. 77, 437–471.

Kjerfve, B., Lacerda, L.Dd, 1993. Mangroves of Brazil. Mangr. Ecosys. Tech. Rep. 2, 245–272.

Kjerfve, B., Perillo, G.M., Gardner, L.R., Rine, J.M., Dias, G.T.M., Mochel, F.R., 2002. Morphodynamics of muddy environments along the Atlantic coasts of North and South America, Muddy Coasts of the World: processes, Deposits and Functions. Elsevier Science, Amsterdam, 479–532.

Körtzinger, A., 2003. A significant sink of CO_2 in the tropical Atlantic Ocean associated with the Amazon River plume. Geophys. Res. Lett. 30 (24), 2287, (doi:2210.1029/2003GL018841).

Kothawala, D.N., Murphy, K.R., Stedmon, C.A., Weyhenmeyer, G.A., Tranvik, L.J., 2013. Inner filter correction of dissolved organic matter fluorescence. Limnol. Oceanogr. Methods 11, 616–630.

Kowalczuk, P., Cooper, W.J., Whitehead, R.F., Durako, M.J., Sheldon, W., 2003. Characterization of CDOM in an organic-rich river and surrounding coastal ocean in the South Atlantic Bight 65. Aquatic Sciences - Research Across Boundaries, 384–401.

Lefèvre, N., Diverrès, D., Gallois, F., 2010. Origin of CO_2 undersaturation in the western tropical Atlantic. Tellus B 62 (5), 595–607, (doi:510.1111/j.1600-0889.2010.00475.x).

Lefèvre, N., Caniaux, G., Janicot, S., Gueye, A.K., 2013. Increased CO_2 outgassing in February-May 2010 in the tropical Atlantic following the 2009 Pacific El Niño. J. Geophys. Res. 118, 1645–1657.

Mehrbach, C., Culberson, C.H., Hawley, J.E., Pytkowicz, R.M., 1973. Measurement of the apparent dissociation constants of carbonic acid in seawater at atmospheric pressure. Limnol. Oceanogr. 18, 897–907.

Mochel, F.R., Ponzoni, F.J., 2007. Spectral characterization of mangrove leaves in the Brazilian Amazonian coast: Turiaçu Bay, Maranhão state. An. Acad. Bras. Cienc. 79, 683–692.

Murphy, K.R., Stedmon, C.A., Waite, T.D., Ruiz, G.M., 2008. Distinguishing between terrestrial and autochthonous organic matter sources in marine environments using fluorescence spectroscopy. Mar. Chem. 108, 40–58.

Noriega, C., Araujo, M., 2014. Carbon dioxide emissions from estuaries of northern and northeastern Brazil. Sci. Rep., 4. http://dx.doi.org/10.1038/srep06164.

Parlanti, E., Wörtz, K., Geoffroy, L., Lamotte, M., 2000. Dissolved organic matter fluorescence spectroscopy as a tool to estimate biological activity in a costal zone submitted to anthropogenic inputs. Org. Geochem. 31, 1765–1781.

Pierrot, D., Lewis, E., Wallace, D.W.R., 2006. MS Excel Program Developed for CO2 System Calculations, In: Carbon Dioxide Information Analysis Center, O.R.N.L., U.S. Department of Energy, Oak Ridge (Ed.), Tennessee.

Pierrot, D., Neill, C., Sullivan, K., Castle, R., Wanninkhof, R., Lüger, H., Johannessen, T., Olsen, A., Feely, R.A., Cosca, C.E., 2009. Recommendations for autonomous underway pCO_2 measuring systems and data-reduction routines. Deep Sea Res. 56, 512–522.

Silva, M., Araujo, M., Servain, J., Penven, P., 2009. Circulation and heat budget in a regional climatological simulation of the southwestern tropical Atlantic. Trop. Oceanogr. 30, 256–269.

Souza-Filho, P.W.M., 2005. Costa de manguezais de macromaré da Amazônia: cenários morfológicos, mapeamento e quantificação de áreas usando dados de sensores remotos. Rev. Bras. De. Geofísica 23, 427–435.

Stedmon, C.A., Bro, R., 2008. Characterizing dissolved organic matter fluorescence with parallel factor analysis: a tutorial. Limnol. Oceanogr. Methods 6, 572–579.

Stramma, L., Schott, F., 1999. The mean flow field of the tropical Atlantic Ocean. Deep Sea Res. II 46, 279–303.

Stubbins, A., Lapierre, J.-F., Berggren, M., Prairie, Y., Dittmar, T., del Giorgio, P., 2014. What's in an EEM? Molecular signatures associated with dissolved organic fluorescence in boreal Canada. Environ. Sci. Technol. 48, 10598–10606.

Sweeney, C., Gloor, E., Jacobson, A.R., Key, R.M., McKinley, G., Sarmiento, J.L., Wanninkhof, R., 2007. Constraining global air-sea gas exchange for CO_2 with recent

bomb 14C measurements. Glob. Biogeochem. Cycles 21. http://dx.doi.org/10.1029/2006GB002784.
Tait, D.R., Maher, D.T., Macklin, P.A., Santos, I.R., 2016. Mangrove pore water exchange across a latitudinal gradient. Geophys. Res. Lett. 43, 3334–3341, (doi: 3310.1002/2016GL068289).
Wada, S., Hama, T., 2013. The contribution of macroalgae to the coastal dissolved organic matter pool. Estuar. Coast. Shelf Sci. 129, 77–85.
Weiss, R.F., 1974. CO_2 in water and seawater: the solubility of a non-ideal gas. Mar. Chem. 2, 203–215.
Xie, P., Janoviak, J.E., Arkin, P.A., Adler, R.F., Gruber, A., Ferraro, R., Huffman, G.J., Curtis, S., 2003. GPCP pentad precipitation analyses: an experimental dataset based on gauge observations and satellite estimates. J. Clim. 16, 2197–2214.
Yamashita, Y., Tanoue, E., 2003. Chemical characterization of protein-like fluorophores in DOM in relation to aromatic amino acids. Mar. Chem. 82, 255–271.
Zhang, Y., van Dijk, M.A., Liu, M., Zhu, G., Qin, B., 2009. The contribution of phytoplankton degradation to chromophoric dissolved organic matter (CDOM) in eutrophic shallow lakes: field and experimental evidence. Water Res. 43, 4685–4697.